Primljen / Received: 1.12.2013.
Ispravljen / Corrected: 3.9.2014.
Prihvaćen / Accepted: 5.10.2014.
Dostupno online / Available online: 10.12.2014.

Numerical modelling of hygrothermal response in building envelopes

Authors:

[1]Assist.Prof. **Mustapha Maliki**
mus27000@yahoo.fr

[1]Assist.Prof. **Nadia Laredj**
nad27000@yahoo.fr

[2,3]Prof. **Hassan Naji**
hassane.naji@univ-artois.fr

[1]Prof. **Karim Bendani**
bendanik@yahoo.fr

[1]Prof. **Hanifi Missoum**
hanifimissoum@yahoo.fr

[1]University Abdelhamid Ibn Badis of Mostaganem, Algeria
Faculty of Science and Technology
"LCTPE Laboratry"

[2]Lille University, France
Civil Engineering & Geo-Environment Laboratory

[3]Artois University, France
Faculty of Applied Sciences

Scientific paper - Preliminary note

Mustapha Maliki, Nadia Laredj, Hassan Naji, Karim Bendani, Hanifi Missoum

Numerical modelling of hygrothermal response in building envelopes

The present paper deals with numerical modelling of heat and mass transfer through multilayer walls. Based on physical principles of mass and energy conservation, nonlinear partial differential equations are developed, where driving potentials are considered. Measurable physical properties involved in the present modelling are dependent on the temperature and capillary pressure, which are considered as driving potentials. A mathematical model that solves the coupled heat and mass transfer through multilayered porous media is developed and validated via a benchmark exercise issued from the HAMSTAD program. The obtained results compare well with benchmark results.

Key words:
Coupled transfer, heat, moisture, multilayer wall, porous media, building simulation

Prethodno priopćenje

Mustapha Maliki, Nadia Laredj, Hassan Naji, Karim Bendani, Hanifi Missoum

Numeričko modeliranje toplinskog odgovora u ovojnicama zgrada

Ovaj rad proučava numeričko modeliranje topline i prijenosa mase kroz višeslojne zidove. Nelinearne parcijalne diferencijalne jednadžbe razvijene su na temelju fizikalnih načela mase i očuvanja energije, a u obzir su uzeti i pripadajući potencijali. Mjerljiva fizikalna svojstva koja su dio modeliranja ovise o temperaturi i kapilarnom tlaku koji se smatraju potencijalima. Matematički model koji rješava prijenos topline i tvari kroz višeslojne porozne medije razvijen je i potvrđen putem referentne vježbe u HAMSTAD programu. Dobiveni rezultati uspoređeni su s referentnim vrijednostima.

Ključne riječi:
kombinirani prijenos, toplina, vlaga, višeslojni zid, porozni medij, simulacija zgrade

Vorherige Mitteilung

Mustapha Maliki, Nadia Laredj, Hassan Naji, Karim Bendani, Hanifi Missoum

Numerische Modellierung des hygrothermischen Verhaltens von Gebäudehüllen

Die vorliegende Arbeit befasst sich mit der numerischen Modellierung von Wärme- und Stoffübertragung in mehrschichtigen Wänden. Auf physikalischen Prinzipen der Massen- und Energieerhaltung beruhend, sind nichtlineare partiale Differenzialgleichungen entwickelt, bei denen treibende Potenziale berücksichtigt sind. Bei der Modellierung einbezogene messbare physikalische Eigenschaften hängen von der Temperatur und dem Kapillardruck ab, die als treibende Potenziale angenommen werden. Ein mathematisches Modell, das die gekoppelte Wärme- und Stoffübertragung in mehrschichtigen porösen Medien beschreibt, ist entwickelt und durch eine Benchmark-Übung im Programm HAMSTAD validiert worden. Die erhaltenen Resultate stimmen gut mit den Referenzwerten überein.

Schlüsselwörter:
gekoppelte Übertragung, Wärme, Feuchte, mehrschichtige Wand, poröse Medien, Gebäudesimulation

1. Introduction

Over the past two decades, the so-called efficient buildings have increasingly made use of multilayered components, which are regarded as innovative technical solutions in the context of energy conservation and sustainable development. Several studies have placed emphasis on the advantages of using renewable materials in the context of energy preservation. However, both thermal and hygroscopic transport must be considered with regard to these materials, so as to accurately predict the heat and moisture transport behaviour, as well as the overall comfort offered by the building. In most recent insulation technologies, the wall itself is made of several different layers. For these envelopes, the heat transfer, moisture transfer, and air infiltration, constitute a typical coupled heat and mass transfer process [1]. An accurate coupled heat, air, and moisture transfer (HAM) through porous media is of special interest in many engineering areas such as in the sphere of pollutants infiltration, drying in porous solids and soils, drying of woods and papers, soil mechanics, thermal insulation for buildings, etc. In this respect, some notable applications are *inter alia* presented in [2-5]. The air infiltration through permeable building elements is of paramount importance in civil engineering applications. In other words, it is an important factor that can considerably affect hygrothermal performance of buildings. The effects of moisture are even more important because the air flow can transport high quantities of water vapour into building elements, which subsequently results in interstitial condensation with a very high condensation rate. This can even lead to serious damage to such permeable and/or leaky elements. In addition, the accumulation of moisture in a material used in building envelopes can lead to poor thermal performance of the envelope, degradation of organic materials, and structural defects. Therefore, detailed heat, air and moisture models must be made with regard to buildings so as to increase the accuracy of defining the heat and moisture transfer between outdoor and indoor environments and, hence, to enable better prediction of thermal loads, indoor thermal comfort, air quality indices, and mould growth hazard.

It should be noted that temperature gradients and water vapour pressure can generate fields of temperature and humidity inside the building envelope. In addition, thermal characteristics and the data on moisture storage levels of the wall should be considered. This combination makes the transport of heat and moisture through the building transient and relatively complex. Despite this complexity, we can numerically simulate the drying-moistening dynamic processes of the building envelope component. In this sense, hygrothermal models have been used to evaluate performance of walls exposed to weather in different geographical locations [6-8]. To describe hygrothermal transfer in the porous capillary media, Luikov [8] uses the analogy between the moisture migration and heat transfer to develop and design a model that uses the temperature and moisture content as driving potentials. Moreover, he assumes that capillary transport is proportional to the moisture and temperature gradients. Also, by analogy to specific heat, he introduces a specific mass capacity, which is defined as the derivative of water content with respect to mass potential. This model can be applied for both hygroscopic and non-hygroscopic materials. It has been used by a number of researchers including [9-11]. Among these authors, we can cite Pedersen [12], who uses the capillary suction pressure, Künzel and Kiessel [13], who consider the relative humidity, and Mendes and Philippi [6], who demonstrate that moisture content gradients can be used as driving forces for the heat and moisture transport calculation for the interface between porous materials with different pore size distribution functions. The calculation approach used by these authors seems correct since it takes into account the discontinuity phenomenon at the interface. Also with regard to the heat transfer through the building envelope, there are some aspects that should be handled using complex calculation. These are the phenomenon's multidimensionality, its transient behaviour, and moisture conditions.

Our main target here is to develop a two-dimensional model to simulate the transfer of heat, air, and moisture in building envelopes. Note that this model belongs to the class of models that have recently emerged to handle the coupled transfer, as mentioned above. These models are used either in commercial codes or house codes to solve problems inherent to buildings physics [14-21].

It should be noted that such models are more flexible for future extensions (e.g. for 2D and/or 3D simulations), because they allow addition of new features, as well as an easy integration with other existing models. One advantage of having a transient heat, air, and moisture model (HAM model) as a whole-building hygrothermal model is that it enables us to capture the potential moisture release from the building surroundings into the indoor space. In fact, moisture sources, from construction and from wet soil, propagating through foundation walls and floor slabs, could take precedence over all internal moisture sources. Similarly, in recent times an emphasis is being placed, when calculating indoor humidity levels, on the importance of quantification of moisture release from foundation slabs. The use of a transient HAM model when conducting the whole-building performance analysis also yields a better estimation of energy demand for heating or cooling of buildings. This is possible due to the fact that transient HAM models take into account the effect of moisture in the heat transfer through building enclosures. When conducting thermal analyses, the energy simulation models usually ignore the effect of moisture [22], and use constant thermal storage and transport property values (thermal conductivity and heat capacity, respectively), despite the fact that these properties can be strongly dependent on moisture content.

It is worth recalling that this paper deals with numerical simulation of the heat, air, and moisture transfer in building systems. The numerical model of the combined heat and moisture transfer, as based on basic functions of partial differential equations (PDEs), is tested in this paper through a benchmark case.

The rest of the paper is structured as follows. The section following this introduction provides a concise description of the physical problem and the mathematical model used in the paper. Section 3 is devoted to boundary conditions of heat and moisture. In Section 4, the model is validated through implementation of a benchmark

case dealing with interstitial condensation that occurs at the contact surface between two materials. The paper ends with some conclusions that summarize our findings.

2. Mathematical modelling

Physical models forming the basis of various software tools that are used to predict the heat, air, and moisture response of building envelopes seem quite diverse. This section addresses the model for heat and moisture transfer through building materials, which has been applied in this paper. It is based on the temperature and capillary pressure, regarded as independent variables.

It should be noted that in the coupled transfer the moisture transport in building materials appears under two different phases: liquid and vapour. The vapour phase is divided into the diffusion and convection parts. Indeed, the diffusive flow of vapour is engendered by the vapour pressure gradient, and the corresponding conductivity represents the permeability of the vapour. As for the convective vapour flow, it is advected by the moving air [22].

The modelling of transfer in the vapour phase by the capillary pressure gradient as conductive potential, and the permeability of liquid as the conductivity of moisture transfer, has become the most appropriate and the most often used approach for this kind of modelling [23]. For the liquid flow, the moisture content gradient has been used in some hygrothermal tools as the driving potential, and the moisture diffusivity as the moisture transfer conductivity.

Governing equations of the coupled transfer in building materials can be formulated according to the principle of preservation of the combined transport of heat and humidity of a representative elementary volume (REV), which is defined as being large enough when compared to pore dimensions, but also small enough compared to the size of the sample.

Different kinds of transport equations and boundary conditions are required in order to simulate the heat and moisture transfer in a multi-layered wall. These equations are outlined below in accordance with the considered medium. The equations require dedicated boundary conditions in order to close the problem and solve the coupled equations. Note that the assumption of ideal gas was made for the dry air and water vapour in order to characterize the humid air mixture.

2.1. Moisture transfer

It should be noted that the moisture transfer through composite walls, even in a one-dimensional process, is a complex phenomenon involving coupled transfer of the liquid, vapour, and heat. According to Qinru et al. [15], and after some manipulations and conjectures, the governing equation for the moisture content through the medium can be expressed by the following equation

$$\partial w/\partial t = \nabla\left(\delta_P \nabla p_V - K_l \nabla p_C\right) - v \cdot \nabla \rho_V + F_{mo} \quad (1)$$

where:

w - moisture content [kg/m³],
t - time [s],
δ_p - water vapour permeability [s],
p_v - partial water vapour pressure [Pa],
K_l - water permeability [s],
p_c - capillary pressure [Pa],
v - air velocity [m/s],
ρ_v - water vapour density [kg/m³],
F_{mo} - moisture source term related to moisture content [kg/m³s].

2.2. Heat transfer

Here, we presume that the main mechanisms governing the transfer of heat are the thermal conduction and convection due to air movement and latent heat. This is due to the presence of low temperature gradients. In this way, the energy conservation equation can be written in terms of driving potentials as follows [24]:

$$\left(c_{P,m}\rho_m + c_{P,l}w\right)\partial T/\partial t = \nabla\left(\lambda \nabla T + L_V \delta_P \nabla p_V\right) - v \cdot \left(L_V \nabla \rho_V + \rho_a c_{P,a} \nabla T\right) + F_h \quad (2)$$

where $c_{P,m}$ [J/kg·K] is the dry specific heat of material, ρ_m [kg/m³] is the dry density of material, $c_{P,l}$ [J/kg·K] is the specific heat of liquid water, w is the moisture content [kg/m³], T [K]is the temperature, λ [W/mK] is the thermal conductivity, L_V [J/kg] is the enthalpy of evaporation, ρ_a [kg/m³] is the dry air density, $c_{P,a}$ [J/kg·K] is the specific heat of dry air, and F_h is the heat source term related to temperature [W/m³].

2.3. Conservation equations and modelling

As stated in the beginning, Eqns (1) and (2) are recast through a single variable which is the capillary pressure (p_c). Moreover, the relationship between the partial water vapour pressure and the relative humidity can be expressed as [15]:

$$p_V = \phi p_{sat} \quad (3)$$

where ϕ is the relative humidity, and p_{sat} [Pa] is the saturated water vapour pressure. Note that the relative humidity is often chosen as flow potential, since it is continuous at the interface of two layers of materials that have different moisture storage properties (sorption and moisture retention). This potential is linked to the capillary pressure via the Kelvin equation:

$$\phi = exp - p_c / (\rho_l R_V T) \quad (4)$$

where ρ_l [kg/m³] is the water density and R_V [J/kg·K] is the gas constant for water vapour.

It results from this that the conservation equations of the combined heat and moisture transfer can be recast in terms of coefficients, and by considering the temperature as an independent variable for heat transfer and the capillary pressure as an independent variable for moisture transfer. By following this procedure, the equations can assume the following form:

$$C_T\left(\partial T/\partial t\right)=\nabla\left(C_{11}\nabla T+C_{12}\nabla p_C\right)+v\cdot\left(D_{11}\nabla T+D_{12}\nabla p_C\right)+F_h \quad (5)$$

$$\Omega\left(\partial p_C/\partial t\right)=\nabla\left(C_{21}\nabla T+C_{22}\nabla p_C\right)+v\cdot\left(D_{21}\nabla T+D_{22}\nabla p_C\right)+F_{mo} \quad (6)$$

where C_T is the specific heat of the medium defined as a function of dry air and liquid water heat capacities ($C_T = c_p\rho + c_{p,l}w$), and Ω [kg/m³Pa] is the moisture storage capacity, defined as the slope of the water retention curve ($\Omega = \partial w/\partial p_c$). It is worth noting that after some manipulations and rearrangements, the above equations (Eqns (5) and (6)) can be written in the following matrix form:

$$d_a\begin{bmatrix}\partial T/\partial t\\ \partial p_C/\partial t\end{bmatrix}=\nabla\left(C\,\nabla\begin{bmatrix}T\\ p_C\end{bmatrix}\right)+\beta\cdot\nabla\begin{bmatrix}T\\ p_C\end{bmatrix}+\begin{bmatrix}F_h\\ F_{mo}\end{bmatrix} \quad (7)$$

where damping (d_a), diffusion (C), and convection (β) matrices are respectively defined by:

$$d_a=\begin{bmatrix}C_T & 0\\ 0 & \Omega\end{bmatrix} \quad (8)$$

$$C=\begin{bmatrix}C_{11} & C_{12}\\ C_{21} & C_{22}\end{bmatrix}=\begin{bmatrix}\lambda+L_V\delta_P\phi p'_{sat} & -L_V\delta_P\phi p_{sat}/\left(\rho_l R_V T\right)\\ -\delta_P\phi p'_{sat} & K_l+\delta_P\phi p_{sat}/\left(\rho_l R_V T\right)\end{bmatrix} \quad (9)$$

$p'_{sat} = \partial p_{sat}/\partial T$ being the derivative of saturation vapour pressure. As for the matrix β, it can be expressed in the following form:

$$\beta=v\cdot\begin{bmatrix}D_{11} & D_{12}\\ D_{21} & D_{22}\end{bmatrix}=v\cdot\begin{bmatrix}-\left[\rho_a c_{P,a}+L_V\left(\partial\rho_V/\partial T\right)\right] & -\left[L_V\phi/\left(\rho_l R_V T\right)\right]\left(\partial\rho_V/\partial\phi\right)\\ \partial\rho_V/\partial T & -\left[\phi/\left(\rho_l R_V T\right)\right]\left(\partial\rho_V/\partial\phi\right)\end{bmatrix} \quad (10)$$

To go further, the current model consists of converting, via MatLab, measurable physical properties of the material such as K_l, ϕ, δ_p and λ dependent on moisture content w into partial differential equations (PDEs), C_{11}, C_{12}, D_{11}, D_{12}, Ω and C_T dependent on p_c and T [25].

3. Boundary conditions (BCs)

It goes without saying that any modelling and numerical simulations have to be backed by appropriate boundary conditions (BCs). In the building envelope simulation, the boundary conditions and initial conditions, carefully selected and combined, greatly help us to achieve good accuracy without resorting to the use of prohibitive computing times. In this framework, external boundary conditions of building envelopes can be divided into three main groups [8, 26], namely the moisture saturation, constant heat and moisture flow, and heat/moisture flow through a surface resistance film applied onto the external surface. External boundary conditions are presented in Eqns (11) and (12). As for the internal surface of the wall, the temperature and pressure are maintained at a constant level.

3.1. Moisture BCs

The supply of moisture flux through the outside surface of the envelope, $g_{n,e}$, can be expressed using the following relationship:

$$g_{n,e} = \beta_{P,e}\,(p_{v,e} - p_{surf,e}) + g_{wdr} \quad (11)$$

where $\beta_{P,e}$ [kg/m²s · Pa] is the vapour transfer coefficient of the exterior surface, $p_{v,e}$ [Pa] is the water vapour pressure of the outdoor air, $p_{surf,e}$ [Pa] is the water vapour pressure at the exterior surface, g_{wdr} [kg/m²s] is the moisture supply due to wind-driven rain. For the internal side of the wall, the moisture flux is obtained according to the following relationship:

$$g_{n,i} = \beta_{P,i}\,(p_{v,i} - p_{surf,i}) \quad (12)$$

where $\beta_{P,i}$ [kg/m²s · Pa] is the vapour transfer coefficient of the interior surface, $p_{v,i}$ [Pa] is the water vapour pressure of the indoor air, and $p_{surf,i}$ [Pa] is the water vapour pressure of the interior surface.

3.2. Heat BCs

Recall that here the heat flux through external surface $q_{n,e}$ [W/m²] includes the effects of conduction, convection, latent heat flow due to vapour, and sensible heat flow due to rain absorption. It can be expressed as:

$$q_{n,e}=\alpha_e\left(T^{eq}-T_{surf,e}\right)+L_V\beta_{p,e}\left(p_{v,e}-p_{surf,e}\right)+g_{wdr}c_{p,l}T^{eq} \quad (13)$$

where α_e [W/m²] is the heat transfer coefficient of the exterior surface, T^{eq} [K] is the equivalent exterior temperature encompassing both the temperatures of the ambient air and that of the solar wave radiation and long wave, and $T_{surf,e}$ [K] is the temperature of the exterior surface.

Likewise, the heat flux through internal surface of the building envelope, $q_{n,i}$ [W/m²], is given by:

$$q_{n,i}=\alpha_i\left(T_i-T_{surf,i}\right)+L_V\beta_{p,i}\left(p_{v,i}-p_{surf,i}\right) \quad (14)$$

where α_i [W/m² · K] is the heat transfer coefficient of the interior surface, T_i [K] is the temperature of indoor air, and $T_{surf,i}$ [K] is the temperature at the interior surface.

It should here be noted that the wind speed in porous media is commonly expressed by the experimentally observed Darcy-Boussinesq law.

$$v=-\frac{k_a}{\mu_a}\nabla p_a \quad (15)$$

where k_a [kg/m·s·Pa] is the air permeability of the material, μ_a [kg/m·s] is the dynamic viscosity of air, p_a [Pa] is the dry air pressure.

3.3. Discretisation, meshing and solver default settings

For spatial discretisation, the system of partial differential equations (PDE) is transformed by COMSOL solver into a set of ordinary differential equations (ODE) through spatial discretisation. The Finite Volume Method (FVM) is used and the computational domain is subdivided into a number of finite elements resulting

in discrete balance equations for all elements. The flux terms are discretised by using central difference approximations for the diffusion terms, and upwinding schemes for the convective terms. An ordinary differential equation system (ODE) is obtained by replacing all spatial gradients with finite difference approximations of the transient heat and moisture balance equations. In the current version of COMSOL, this system of combined heat and moisture transport is solved using the Newton-Raphson iteration method implemented in the generic ODE-solver. The implementation of this generic multi-step solver in the COMSOL framework is extensively documented in [27]. However, since the air mass balance equation is simplified to a steady state formulation, its discretised form cannot be included in the general form of the obtained ordinary differential equation. Therefore, this set of linear equations is solved separately from the coupled transient heat and moisture transport. In this respect, the quasi-steady state implementations means that the air flow field is kept constant during integration of the coupled energy and moisture balance equations. At defined time intervals, a new steady state solution of the air flow field is calculated and used during the continued integration of heat and moisture balances.

Using meshes that smoothly change in size near the interface of two internal layers, where the solution is expected to change abruptly, a regular 157-node mesh has been applied, which resulted in 216 triangular elements.

It should also be noted that some default settings were selected for the COMSOL solver parameters. Linear time dependent system solver called UMFPACK, as a set of routines for solving unsymmetrical sparse linear systems, was selected. Also, a shape function denoted SHLAG (Lagrange element of second order) was adopted for both temperature and capillary pressure. A variable time step was chosen, which enabled fast convergence.

4. Numerical handling and validation of the model

4.1. One dimensional benchmarking case

As stated above, the adequacy of the aforementioned model equations has been checked considering a 1D benchmark exercise #1. The latter arises from a series of benchmark cases based on the EU-initiated project for the standardization of heat, air and moisture calculation methods (European project known as HAMSTAD-WP2) [28, 29]. Five exercises from this benchmark assessment are appropriate for assessing the performance and accuracy of hygrothermal models in one dimensional configuration. In this project, Hagentoft et al. [29] developed a model in which they considered the temperature and the capillary suction pressure (or partial water vapour pressure), as potentials for the energy conservation and moisture transport, respectively.

The benchmark exercise presented in Figure 1 deals with interstitial condensation occurring at the contact surface between two materials. The structure, from the lowest x-coordinate (external side) to the highest one, is composed of: the air and vapour tight seal, 100 mm load bearing material, and 50 mm thermal insulation, cf. Figure 1. The materials have different thermal and moisture properties: the load bearing material is capillary active, and the insulation is hygroscopic but capillary inactive (infinite resistance to liquid flow). Their thermal conductivities differ by the factor of 50 (in dry conditions). The structure is perfectly airtight. Note that other benchmarking exercises also exist, as reported in Tariku [30].

4.1.1. Material property functions

Material properties in terms of moisture content *w* are given below for both the bearing layer and insulation, respectively. Some thermo-physical specifications of materials are presented in Table 1.

Load bearing material

Water retention curve:

$$w = \frac{146}{\left(1+\left(8\cdot 10^{-8}\cdot p_C\right)^{1.6}\right)^{0.375}} \quad [\mathrm{kg/m^3}]$$

$$p_C = 0.125\cdot 10^8\left(\left(\frac{146}{w}\right)^{\frac{1}{0.375}}-1\right)^{0.625} \quad [\mathrm{Pa}]$$

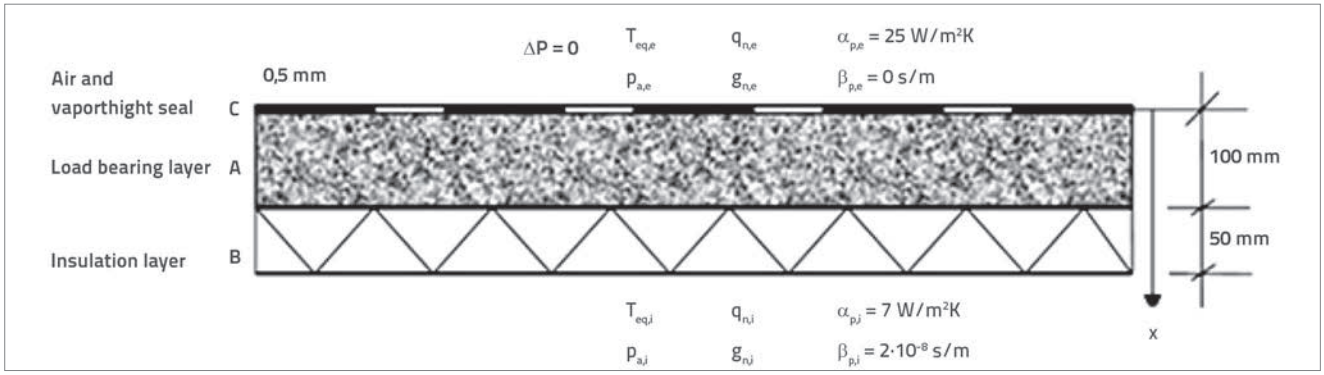

Figure 1. Construction details for the analysed benchmark case

Sorption isotherm:

$$w = \frac{146}{\left(1+\left(-8\cdot10^{-8}\cdot\frac{RT\rho_w}{M_w}\ln(\phi)\right)^{1.6}\right)^{0.375}} \quad [kg/m^3]$$

$$\phi = \exp\left(-\frac{M_w}{RT\rho_w}0.125\cdot10^8\left(\left(\frac{146}{w}\right)^{\frac{1}{0.375}}-1\right)^{0.625}\right)$$

Vapour diffusion:

$$\delta_p = \frac{M_w}{RT}\cdot\frac{26.1\cdot10^{-6}}{200}\cdot\frac{1-\frac{w}{146}}{0.503\cdot\left(1-\frac{w}{146}\right)^2+0.497} \quad [s]$$

Liquid water permeability:

$$K = \exp(-39.2619+0.0704\cdot(w-73)-1.7420\cdot10^{-4}\cdot(w-73)^2 - 2.7953\cdot10^{-6}\cdot(w-73)^3-1.1566\cdot10^{-7}\cdot(w-73)^4 + 2.5969\cdot10^{-9}\cdot(w-73)^5) \quad [s]$$

Thermal conductivity:

$$\lambda = 1.5+\frac{15.8}{1000}w \quad [W/mK]$$

Heat capacity of dry material:

$\rho_0 c_0 = 1.824 \cdot 10^6$ [J/m³K]

Insulating material

Water retention curve:

$$w = \frac{900}{\left(1+\left(2\cdot10^{-4}\cdot p_c\right)^2\right)^{0.5}} \quad [kg/m^3]$$

$$p_c = 0.5\cdot10^4\left(\left(\frac{900}{w}\right)^2-1\right)^{0.5} \quad [Pa]$$

Sorption isotherm

$$w = \frac{900}{\left(1+\left(-2\cdot10^{-4}\cdot\frac{RT\rho_w}{M_w}\ln(\phi)\right)^2\right)^{0.5}} \quad [kg/m^3]$$

$$\phi = \exp\left(-\frac{M_w}{RT\rho_w}0.5\cdot10^4\left(\left(\frac{900}{w}\right)^2-1\right)^{0.5}\right)$$

Vapour diffusion:

$$\delta_p = \frac{M_w}{RT}\cdot\frac{26.1\cdot10^{-6}}{9.6}\cdot\frac{1-\frac{w}{900}}{0.503\cdot\left(1-\frac{w}{900}\right)^2+0.497} \quad [s]$$

Liquid water permeability:

$K = 0$ [s]

Thermal conductivity:

$$\lambda = 0.033+\frac{0.59}{1000}w \quad [W/mK]$$

Heat capacity of dry material:

$\rho_0 c_0 = 0.0739 \cdot 10^6$ [J/m³ · K]

Table 1. Some general data about materials

Thermo-physical parameter	Symbol	Unit	Value
Liquid water density	ρ_w	kg/m³	1000
Gas constant for water vapour	R	J/molK	8,314
Molar mass of water vapour	M_w	kg/mol	0,018
Enthalpy of evaporation	L_V	J/kg	$2{,}5\cdot10^6$

4.1.2. Initial conditions

The following initial conditions were adopted:
- For load bearing material: w = 145 kg/m³; T = 283 K
- For insulation: w = 0.065 kg/m³; T = 283 K.

4.1.3. Boundary conditions

The applied boundary conditions corresponding to the problem under study are fixed temperature and humidity (Dirichlet boundary conditions) :
- A data file supplies hourly values for heat and moisture for a period of more than one year. Intermediate values of time are obtained by interpolation.
- No difference in pressure is considered.

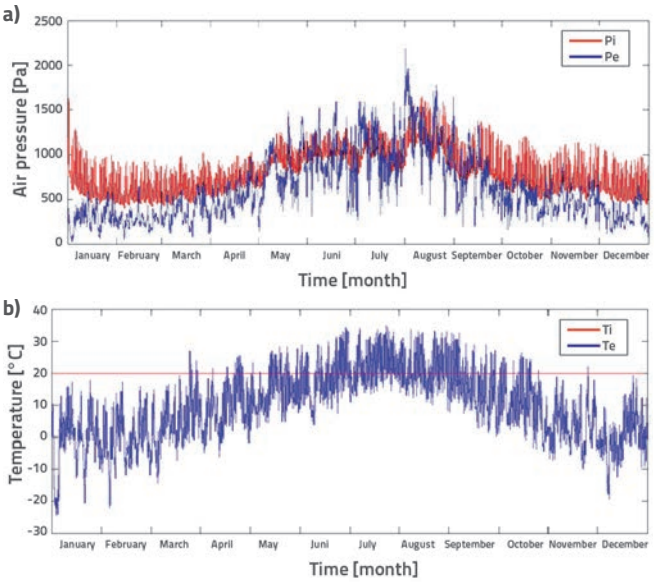

Figure 2. Boundary conditions for the simulation period (one year): a) external and internal air pressure; b) external and internal ambient temperature

Figure 2 shows climatic conditions for a period of one year representing duration of simulation process. These conditions consist of:

- The outside equivalent temperatures T_e and internal temperature T_i, which is set to 20°C in order to ensure an optimum interior thermal comfort.
- External and internal air pressure variations P_e and P_i.

The surface transfer coefficients are given by:

$\alpha_{e,e} = 25$ [W/m²K], $\alpha_{e,i} = 7$ [W/m²K]

$\beta_{p,e} = 0$ [s/m], $\beta_{p,i} = 2 \cdot 10^{-8}$ [s/m]

Note that these conditions allow for a very good case for checking the heat and moisture transfer model.
It has already been mentioned that the numerical simulation was performed using the COMSOL Multiphysics software (CMS) [31], and the required results are:

- Capillary pressure p_c, in space and time for the load bearing layer A, and insulation B.
- Temperature T(x,t) .
- Total moisture weight M in each layer.
- Heat flux q crossing the structure from interior to the wall.

The model simulated, for the period of more than one year, the distribution of the capillary pressure p_c and the temperature T. The temperature and capillary pressure distribution in the load bearing layer and insulation is depicted in Figure 3.

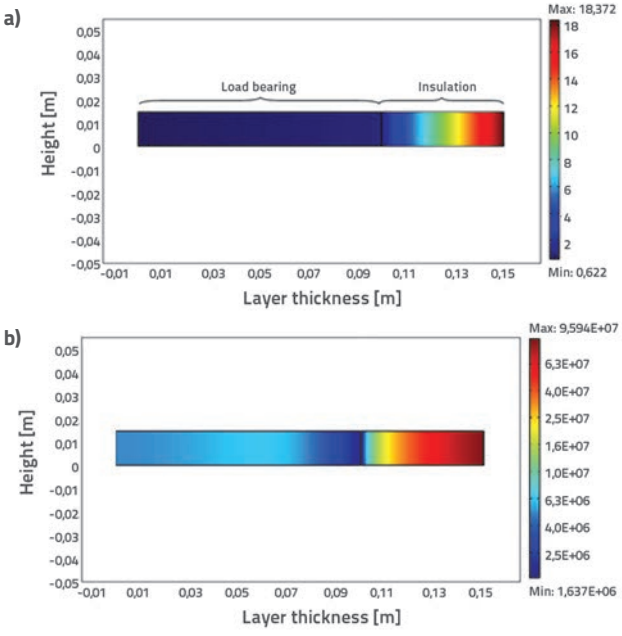

Figure 3. Distribution variables in the wall after 86400 hours: a) Temperature T [°C]; b) Capillary pressure p_c [Pa]

4.1.4. Results and discussion

Moisture transport

Using properties of the material, the total moisture content can easily be computed from the distribution of capillary pressure p_c. Figure 4 shows the total moisture content in the load bearing layer during one year. An important increase in moisture content was observed as a result of the low average external temperature (-3 °C) in winter period, and the convection implying mass displacement front towards the lower air pressure (Figs. 2.a and 2.b). Conversely, dry conditions occurring between 2500 and 6500 hours, and a weak convection effect, caused an abrupt drying of the material. High discrepancies between the internal and external pressure, coupled with the temperature drop, were observed during the last quarter of the simulation period, which lead to a new increase in the moisture content levels. A comparison between the current model results and the HAMSTAD test results was conducted. It can be seen that the predicted profile generally corroborates, over the considered period, HAMSTAD's results with an average difference evaluated to 1.65% only. This allows us to state that results available in literature can be reproduced by the current model.

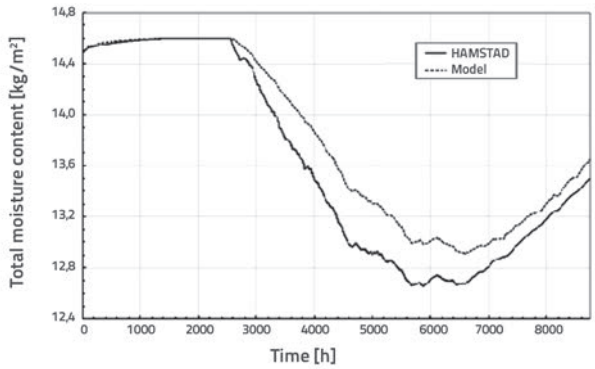

Figure 4. Time-dependent change of total moisture content in load bearing layer during the first year

Heat transport

The heat flow crossing the structure from the inside during the first 500 hours, as obtained with the current model in comparison with the HAMSTAD test, is shown in Figure 5. The graph tendency of the heat flux depends on the period of the day; the quantity of energy crossing the wall is inversely proportional to the outside temperature. Indeed, the ascending tendency corresponds to the period of the day between 3 pm and 8 am when the average temperature is globally negative, with the maximum outgoing flux registered at about 8 am. The downward part of the graph represents the flux behaviour during the rest of the day, when the average temperature is globally positive, and when the lowest heat flux value is registered at 3 pm.
This figure shows that prediction of the model is very close to that of the test case. Moreover, some registered peaks suggest a possible numerical instability. At this point, it is emphasized that all results were obtained using default settings of the grid and

solvers. Even better results can be expected if more attention is paid to these settings. This will further be elaborated in future research.

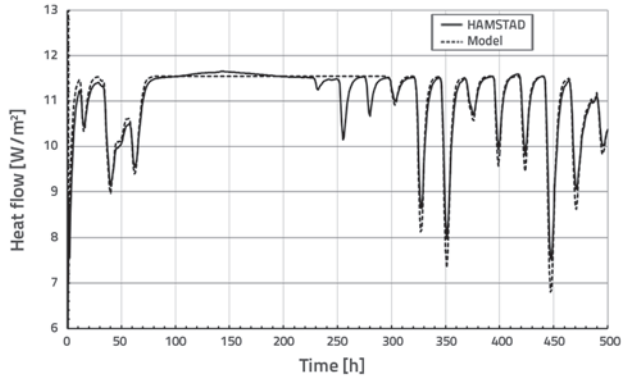

Figure 5. Time-dependent change of heat flux from interior to the wall

To investigate energy distribution within the studied structure, the temperature variation through the studied structure, presented in Figure 1 at the end of each of first three days of the year, respectively, is depicted in Figure 6. The measurements show that the temperature gradient is maximum in the insulating material where the regulating effect of heat is strongly proven. The registered outer surface temperatures corresponding to the three cases are 0,52 °C, 0,63 °C, and 2,87 °C, respectively. The temperature within the load bearing layer remains quasi constant. This is due to the very high thermal conductivity of the material and the predominance of convective terms in the porous material, which is implicitly considered by the present model. It should also be noted that the gradient of temperature calculated in the insulating material is about one hundred times superior to that registered in the load bearing layer.

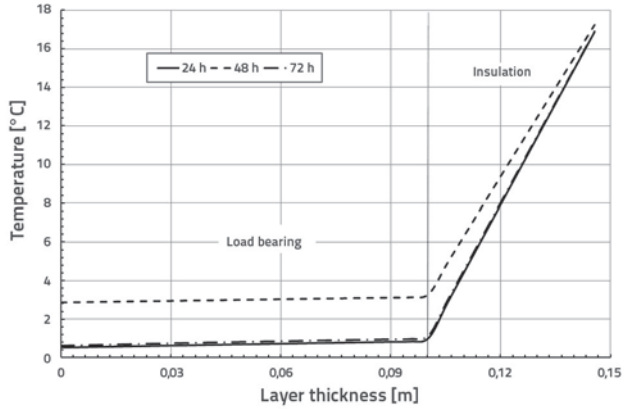

Figure 6. Temperature distribution through both layers at 24, 48 and 72 hours

The temperature evolution profile during the first 72 hours, at different positions of the multilayered structure, is shown In Figure 7. Three curves at the bottom of the graph, expressing temperature fluctuations at three different points of the load bearing layer, are almost similar. The high conduction and convection of the material makes the temperature almost constant. This also explains the vertiginous fall of temperature during the first ten hours, when the temperature falls from 283 K (initial temperature of the structure) to about 274 K (outside ambient temperature). Thermal behaviour of the load bearing layer reflects the outside ambient temperature variations.

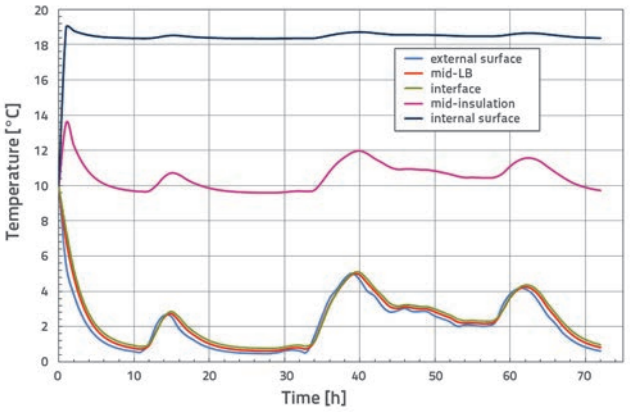

Figure 7. Time-dependent change of temperature at different positions

Paradoxically, the temperature in the middle of the insulating material represents approximately one half of the temperature difference between the inside and outside surfaces. The insulating material used ensures after half an hour, for the interior surface, a relatively constant temperature bordering the internal ambient temperature (20 °C).

5. Conclusion

A combined HAM transport model for consolidated porous buildings materials is presented. The model considers the capillary pressure and temperature gradients as driving potentials of the coupled heat and moisture transfer through porous materials of a building envelope. This model is successfully benchmarked against two test cases. The governing partial-differential equations of three transport phenomena are coupled and solved simultaneously for a given temperature and capillary pressure, the latter being considered as the relevant variable. The COMSOL solver is the code chosen to solve governing equations for HM transport. A good agreement with the considered benchmarks evidences the potential of the present model, and suggests that its development and implementation are promising, and thus, that it can be further coupled with an indoor model to create a whole building hygrothermal model, taking into account the multi-dimensional heat, air, and moisture transfer.

The implementation of this model, and its validation through other benchmark studies, are in progress. As a final conclusion, it can be stated that the approach used in this paper provides a reliable and efficient model for simulating the coupled heat, air, and moisture transfer through multilayer building elements.

REFERENCES

[1] Lin, M.W., Berman, J.B.: Modelling of moisture migration in an FRP reinforced masonry structure, *Building and Environment*, 41, pp. 646-656, 2006, doi: 10.1016/j.buildenv.2005.02.026

[2] Awadalla, H.S.F., El-Dib, A.F., Mohamad, M.A.: Mathematical modelling and experimental verification of wood drying process, *Energy Conversion and Management*, 45, pp. 197-207, 2004, doi: 10.1016/S0196-8904(03)00146-8

[3] Ingham, D.B., Pop, I.: *Transport Phenomena in Porous Media*, Elsevier, Oxford,2005.

[4] Olutimayin, S.O., Simonson, C.J.: Measuring and modeling vapor boundary layer growth during transient diffusion heat and moisture transfer in cellulose insulation, *International Journal of Heat and Mass Transfer*, 48, pp. 3319–3330, 2005, doi: 10.1016/j.ijheatmasstransfer.2005.02.024

[5] Osanyintola, O.F., Simonson, C.J.: Moisture buffering capacity of hygroscopic building materials: experimental facilities and energy impact, *Energy and Buildings*, 38, pp. 1270-1282, 2006, doi: 10.1016/j.enbuild.2006.03.026

[6] Mendes, N., Philippi, P.C.: A method for predicting heat and moisture transfer through multilayered walls based on temperature and moisture contents gradients, *International Journal of Heat and Mass Transfer*, 48, pp. 37-51, 2005, doi: 10.1016/j.ijheatmasstransfer.2004.08.011

[7] Philip, JR., De Vries, D.A.: Moisture movement in porous materials under temperature gradients, *Trans. Am. Geophys. Union, Transactions, American Geophysical Union*, 38(2), pp. 222-232, 1957, doi: 10.1029/TR038i002p00222

[8] Luikov, AV.: *Heat and Mass Transfer in Capillary porous Bodies (Chap. 6)*, Pergamon Press, Oxford, UK, 1966.

[9] Mendes, N., Philippi, P.C., Lamberts, R.: A new mathematical method to solve highly coupled equations of heat and mass transfer in porous media, *International Journal of Heat and Mass Transfer*, 45, pp. 509-518, 2002, doi: 10.1016/S0017-9310(01)00172-7

[10] dos Santos, G.H., Mendes, N.: Unsteady combined heat and moisture transfer in unsaturated porous soils, *Journal of Porous Media*, 5, pp. 493-510, 2005, doi: 10.1615/JPorMedia.v8.i5.70

[11] dos Santos, G.H., Mendes, N.: Heat, air and moisture transfer through hollow porous blocks, *International Journal of Heat and Mass Transfer*, 52(9-10), pp. 2390-2398, 2009, doi: 10.1016/j.ijheatmasstransfer

[12] Pedersen, C.R.: Prediction of moisture transfer in building constructions, *Building and Environment*, 27(3), pp. 387-397, 1992, doi: 10.1016/0360-1323(92)90038-Q

[13] Künzel, H.M., Kiessel, K.: Calculation of heat and moisture transfer in exposed building components, *International Journal of Heat and Mass Transfer*, 40(1), pp. 159-167, 1997, doi: 10.1016/S0017-9310(96)00084-1

[14] Kalagasidis, A.S.: *HAM-Tools: an integrated simulation tool for heat, air and moisture transfer analyses in building physics*, PhD Dissertation. Chalmers University of Technology, Gothenburg, Sweden, 2004.

[15] Qinru, Li, Jiwu, R., Fazio, P.: Development of HAM tool for building envelope analysis, *Building and Environment*, 44 (5), pp. 1065-1073, 2009, doi: 10.1016/j.buildenv.2008.07.017

[16] Qin, M., Belarbi, R., Aït-Mokhtar, A., Nilsson, L.O.: Coupled heat and moisture transfer in multi-layer building materials, *Construction and Building Materials*, 23 (2), pp. 967-975, 2009, doi: 10.1016/j.conbuildmat.2008.05.015

[17] Qin, M., Aït-Mokhtar, A., Belarbi, R.: Two-dimensional hygrothermal transfer in porous building materials, *Applied Thermal Engineering*, 30 (16), pp. 2555-2562, 2010, doi: 10.1016/j.applthermaleng.2010.07.006

[18] Kong, F., Wang, H.: Heat and mass coupled transfer combined with freezing process in building materials: Modeling and experimental verification, *Energy and Buildings*, 43 (10), pp. 2850-2859, 2011, doi: 10.1016/j.enbuild.2011.07.004

[19] Ramos, N.M.M., Kalagasidis, A.S., de Freitas, V.P., Delgado, J.M.P.Q.: Numerical simulation of transient moisture transport for hygroscopic inertia assessment, *Journal of Porous Media*, 15(8), pp. 793-804, 2012, doi: 10.1615/JPorMedia.v15.i8.80

[20] Klemczak, B.: Prediction of Coupled Heat and Moisture Transfer in Early-Age Massive Concrete Structures, *Numerical Heat Transfer, Part A: Applications*, 60(3), pp. 212-233, 2011, doi: 10.1080/10407782.2011.594416

[21] Woloszyn, M., Rode, C.: Tools for performance simulation of heat, air and moisture conditions of whole buildings, *Building Simulation*, 1(1), pp. 5-24, 2008, doi: 10.1007/s12273-008-8106-z

[22] Tariku, F., Kumaran, M.K., Fazio, P.: Transient model for coupled heat, air and moisture transfer through multilayered porous media, *International Journal of Heat and Mass Transfer*, 53 (15-16), pp. 3035-3044, 2010, doi: 10.1016/j.ijheatmasstransfer.2010.03.024

[23] Carmeliet, J., Hens, H., Roels, S., Adan, O., Brocken, H., Cerny, R., Pavlik, Z., Hall, C., Kumaran, K., Pel, L.: Determination of the liquid water diffusivity from transient moisture transfer experiments, *Journal of Thermal Envelope and Building Science*, 27(4), pp. 277-305, 2004, doi: 10.1177/1097196304042324

[24] Thomas, H.R., Missoum, H.: Three-dimensional coupled heat, moisture, and air transfer in a deformable unsaturated soil, *International Journal for Numerical Methods in Engineering*, 44(7), pp. 919–943, 1999, doi: 10.1002/(SICI)1097-0207(19990310)44:7<919::AID-NME535>3.0.CO;2-C

[25] van Schijndel, A.W.M.: *Integrated Heat Air and Moisture Modeling and Simulation*, PhD. Dissertation, Eindhoven University of Technlogy, Eindhoven, Netherlands, 2007.

[26] Künzel, H.M.: *Simultaneous heat and moisture transport in building components: one and two-dimensional calculation using simple parameters*, PhD Thesis, Institute of Building Physics, Germany, 1995.

[27] Nicolai, A.: Modelling and numerical simulation of salt transport and phase transitions in unsaturated porous building materials, PhD. dissertation, Syracuse University, New York, 2007.

[28] Hagentoft, C.E.: HAMSTAD – Final report: Methodology of HAM-modeling. Report R-02:8. Gothenburg, Department of Building Physics, Chalmers University of Technology, 2002.

[29] Hagentoft, C.E., Kalagasidis, A.S., Adl-Zarrabi, B., Roels, S., Carmeliet, J., Hens, H., Grunewald, J., Funk, M., Becker, R., Shamir, D., Adan, O., Brocken, H., Kumaran, K., Djebbar, R.: Assessment Method of Numerical Prediction Models for Combined Heat, Air and Moisture Transfer in Building Components: Benchmarks for One-dimensional Cases, *Journal of Thermal Envelope and Building Science*, 27(4), pp. 327-352, 2004, doi: 10.1177/1097196304042436

[30] Tariku, F.: *Whole building heat and moisture analysis*, PhD. Thesis, Concordia University, Montreal, Canada, 2008.

[31] Comsol, Multiphysics Modeling and Simulation Software, <http://www.comsol.com>,2011.